

# Efficient Inter-Channel Interference Monitoring using DSP in Standard Coherent Receivers

Leonardo Minelli,<sup>1,\*</sup> Gabriella Bosco,<sup>1</sup> Antonino Nespola,<sup>2</sup> Stefano Straullu,<sup>2</sup> Stefano Piciaccia<sup>3</sup> and Dario Pileri<sup>1</sup>

<sup>1</sup> DET, Politecnico di Torino, C.so Duca degli Abruzzi 24, Torino, Italy

<sup>2</sup> LINKS Foundation, Via Pier Carlo Boggio 61, Torino, Italy

<sup>3</sup> Cisco Photonics Italy S.r.l., Via Santa Maria Molgora 48/C, Vimercate, Italy

\*leonardo.minelli@polito.it

**Abstract:** We experimentally demonstrate an efficient Optical Performance Monitoring algorithm, based on a Machine Learning-assisted Digital Signal Processing scheme suitable for standard coherent receivers, for estimating asymmetric cross-talk between adjacent WDM channels. © 2024 The Author(s)

## 1. Introduction

Modern optical networks require higher spectral efficiency in order to increase their effective capacity. This can be achieved by using flexible Wavelength Division Multiplexing (WDM) grids, together with tight spacing between channels [1]. Consequently, for a given channel in the WDM comb, it becomes fundamental to accurately estimate the frequency spacing from the adjacent channels: in this way it is possible to jointly maximize the use of the available spectrum and avoid the Inter-Channel Interference (ICI) caused by a partial overlap between channels. Optimal WDM channel spacing estimation can be achieved by exploiting Optical Spectrum Analyzers (OSAs). However, the widespread OSA adoption at every transceiver is discouraged due to cost reasons. Therefore, a better approach is to exploit Digital Signal Processing (DSP) algorithms within standard coherent receivers (RX) to estimate ICI at every stage of an optical network.

Various ICI monitoring DSP techniques have been proposed, exploiting either the equalizer coefficients [2] or the equalized samples [3, 5]. However, the performance of those methods can be affected by a partial loss of ICI information in the previous DSP chain. Furthermore, they lack the capability to determine the specific location (i.e., left and/or right within the spectrum) of the interfering channels. In this work, we propose a DSP scheme for Inter-Channel Interference-Optical Performance Monitoring (ICI-OPM), which directly processes the raw Analog-to-Digital Converter (ADC) samples in the coherent RX to accurately estimate the position of the neighboring WDM channels, exploiting an Artificial Neural Network (ANN). This scheme may be implemented offline (i.e. using an external board that periodically processes a block of ADC samples), or integrated in timing recovery schemes, since they are usually based on band-pass filtering of ADC samples along the spectral edges [6]. Experimental results using commercial coherent transceivers at 52 Gbaud show that the distance from the neighboring WDM channels can be estimated with a Root Mean Square Error (RMSE) of less than 1.5 GHz.

## 2. Methodology

In this work, we demonstrate the proposed ICI-OPM technique over a flexible-grid WDM system, with Root-Raised Cosine (RRC) shaped channels, as illustrated in Fig. 1(a). We quantify the ICI in terms of guard-band between the Channel Under Test (CUT) and its neighboring Left Interfering Channel (LIC) and Right Interfering Channel (RIC)

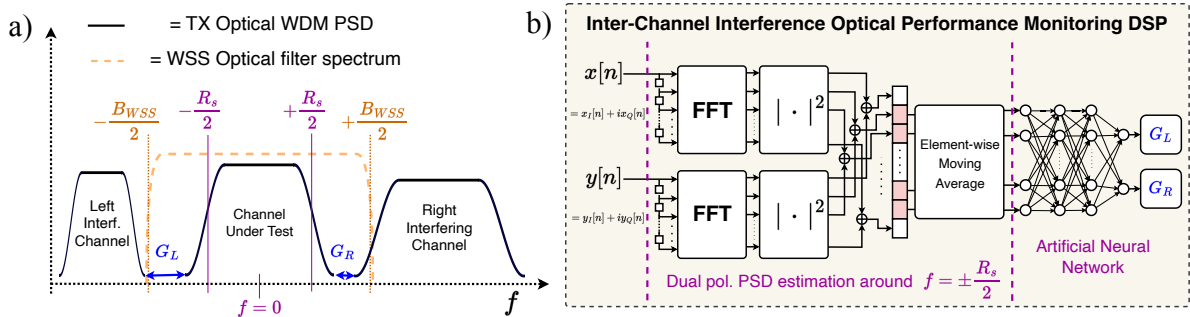


Fig. 1: a) Optical Spectrum of the considered 3-channel WDM system. b) Block scheme of the proposed ICI-OPM DSP.

Channel (RIC). The guard-band is defined as the frequency difference between the end of the spectral support of the CUT and the beginning of the LIC or RIC spectra (respectively,  $G_L$  and  $G_R$ , as shown in Figure 1(a)). We propose a DSP+ANN scheme, which directly estimates  $G_L$  and  $G_R$  from the raw ADC samples of a commercial coherent RX: the related block scheme is depicted in Fig. 1(b). We define  $x[n] = x_I[n] + ix_Q[n]$  and  $y[n] = y_I[n] + iy_Q[n]$ , as, respectively, the X and Y polarization complex signal samples generated by the RX ADC, where  $n$  denotes the discrete time index and  $I$  and  $Q$  indicate the in-phase and quadrature components. To provide a single  $G_L$  and  $G_R$  estimation, the DSP scheme processes 2048 consecutive samples of  $x[n]$  and  $y[n]$ . First, it estimates the dual-polarization Power Spectral Density (PSD)  $S[n] = S_X[n] + S_Y[n]$  (i.e., the sum of the PSD over the X and Y polarizations  $S_X[n]$  and  $S_Y[n]$ ). The PSD calculation is implemented using a Bartlett periodogram with a FFT window of 256 samples [7]. The computation is performed only within two spectral regions, spanning 110 consecutive frequency bins and centered around half of the CUT symbol rate (i.e. around  $f = \pm R_s/2$ , see Fig. 1(a)). By confining the computation to these specific regions rather than to the entire spectrum, we reduce the complexity of the Bartlett implementation. Moreover, this also allows the algorithm to be potentially integrated with FFT-based clock-recovery algorithms [6].

The computed spectral data is subsequently fed into an ANN. Employing Stochastic Gradient Descent (SGD) optimization, the neural network is trained to map the provided spectral shapes into estimations of both left and right guard-bands  $G_L$  and  $G_R$ . In our experiments (see Sec. 4) a standard Feed-Forward structure with two 25 neurons-hidden layers and Leaky ReLU activation function was sufficient to achieve optimal results: no significant improvements were observed through the use of more advanced (and complex) architectures.

### 3. Experimental Setup

The ICI-OPM DSP scheme was experimentally validated with the setup of Fig. 2(a). We used a set of commercial coherent transceivers (CISCO NCS-1004) to transmit a 3-channel WDM signal (i.e., the CUT, the LIC and the RIC) in a back-to-back setup, optionally using a Wavelength Selective Switch (WSS) to induce an filtering penalty on the CUT. The performance was evaluated in five distinct WSS optical filtering scenarios. These include one scenario where the WSS was not applied, and four scenarios where the WSS was employed with different bandwidths (denoted as  $B_{WSS}$ , see Fig. 1(a)). For each considered scenario, to train and test the ANN-based scheme, 200 different WDM channel configurations were measured, with each acquisition made of  $2^{17}$  ADC samples sequences (X/Y polarization and I/Q phase) from the coherent RX relative to the CUT ( $f_{ADC}=96$  GHz). For each configuration, the CUT spectrum had a fixed roll-off equal to 0.2, and the OSNR was set to 17 dB. The interfering WDM channels were configured with the same symbol rate as the CUT channel (52 Gbaud), but they featured an asymmetric variation of the guard-bands values  $G_L$  and  $G_R$  between  $-13$  GHz and  $16$  GHz (negative values correspond to a partial overlap between interfering channel and CUT). Moreover, variations were introduced in both the LIC and the RIC signals, to efficiently cover a broad range of conditions and spectral shapes, thus emulating a flexible WDM scenario. Specifically, their roll-off was uniformly varied between 0.1 and 0.3, and their relative power (with respect to the power of the CUT) between  $+3$  dB and  $-3$  dB, keeping the total received power constant.

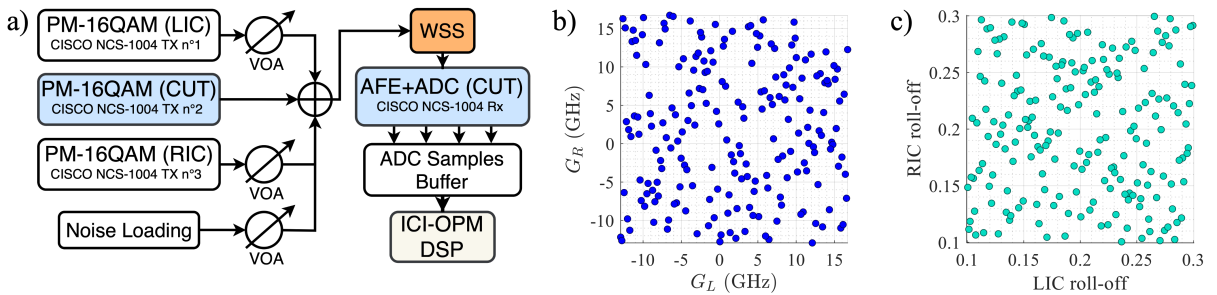


Fig. 2: a) Experimental Setup; b,c) LHS sampled points for guard-band and roll-off values. AFE: Analog Front-End

To design a suitable and efficient dataset, spanning the entire parameter space, with the constraint of 200 configurations, we used Latin Hypercube Sampling (LHS) with an emphasis on minimizing correlation [8]. Using LHS (see e.g. Figs. 2(b) and 2(c)), each of the 200 configurations had unique values for all the considered parameters (guard-band, roll-off, and relative power). Then, training and test of the ANN-based DSP were performed through  $k$ -folding with  $k=10$  over all the configurations. For each fold, the training process involved iteratively propagating through the ANN-based DSP scheme, for 50000 times,  $60 \times 4 \times 2048$  consecutive ADC samples randomly sampled from the train dataset (60 refers to the batch size, 4 to the X/Y and I/Q components). At each iteration, using gradient back-propagation, a Mean Square Error (MSE) loss on the estimated  $G_L$  and  $G_R$  values was then employed to update the ANN coefficients through SGD (using Adam optimizer, with learning rate  $\varepsilon = 0.001$ ).

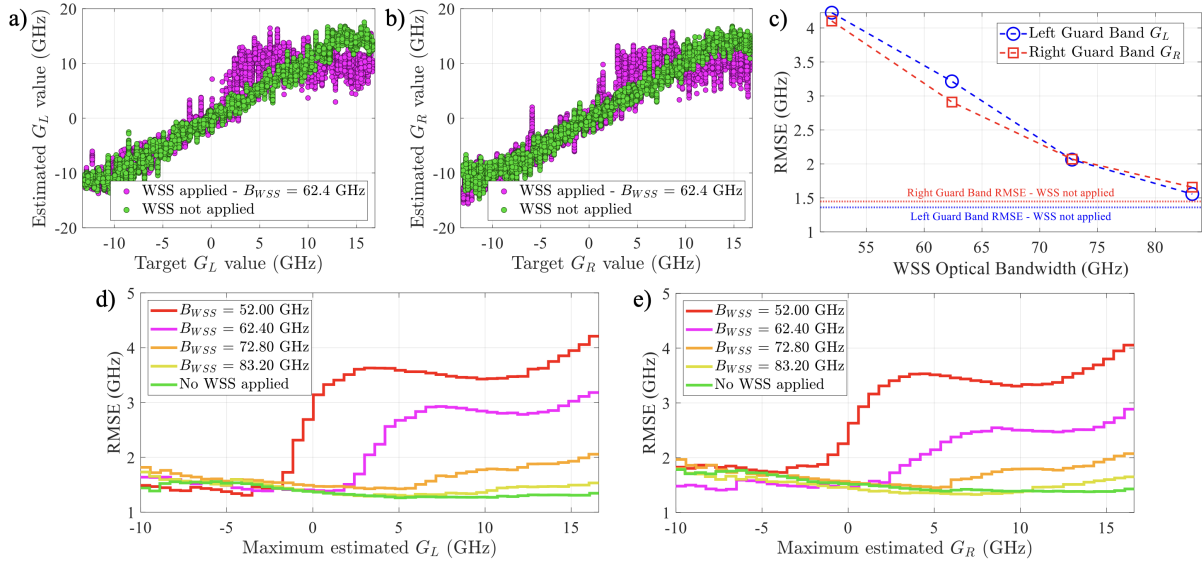


Fig. 3: Experimental results using the ICI-OPM DSP scheme. a,b) left and right guard-band estimation scatter plot; c) RMSE performance as function of  $B_{WSS}$ ; d,e) RMSE performance as function of maximum estimated guard-band.

#### 4. Experimental Results

The ICI-OPM results from the acquired experimental dataset using the proposed DSP algorithm are illustrated in Fig. 3. Figs. 3(a) and 3(b) show that the proposed algorithm is able to effectively estimate both the left and the right guard-bands. Higher values of  $G_L$  and  $G_R$  are correctly estimated without WSS filtering (green dots); in the case of tight optical filtering (violet dots), the guard-band estimation degrades as the WSS optical filtering cancels out the interfering channels. Fig. 3(c) shows the overall (i.e., averaged over the k-folded test dataset) Root Mean Square Error (RMSE) performance in the considered optical filtering scenarios: without WSS filtering (horizontal dotted lines), the algorithm is capable of accurately estimating the guard-bands with an RMSE below 1.5 GHz for both  $G_L$  and  $G_R$ . The RMSE then progressively increases as the WSS bandwidth  $B_{WSS}$  decreases. Nevertheless, the overall performance degradation is strictly dependent on the values of guard-band the ICI-OPM algorithm targets to estimate. In this regard, Fig. 3(d) and 3(e) illustrate the RMSE evolution as a function of the maximum estimated guard-band value. It is evident that the cross-talk (corresponding to negative guard-band values) is well estimated in all the scenarios, while the estimation degrades only when trying to estimate guard-band values beyond the available bandwidth of the RX signal (which is strictly limited by the WSS bandwidth). Therefore, provided that the optical filtering is not severe (such as considering  $B_{WSS}=52$  GHz, see red curves in Figure 3(d,e)), the proposed DSP solution can effectively address ICI-OPM.

#### 5. Conclusion

In this paper, we proposed an ANN-based DSP algorithm able to effectively estimate the location of neighboring interfering channels in a flexible WDM system, using the raw ADC samples captured by a commercial transceiver. Experimental results show that the scheme is effective in predicting the guard band between the channel under test and the neighboring channels over a wide range of conditions, with an estimation accuracy up to 1.5 GHz RMSE.

**Acknowledgments** This work was carried out in the PhotoNext Center at Politecnico di Torino ([www.photonext.polito.it](http://www.photonext.polito.it)) under a research program with Cisco Photonics. It was also partially sponsored by the European Union under the Italian National Recovery and Resilience Plan (NRRP) of NextGenerationEU, partnership on 'Telecommunications of the Future' (PE00000001 - program 'RESTART').

#### References

1. A. Lord et al., "Flexible Technologies to Increase Optical Network Capacity," *Proc. IEEE*, 110 (11), 1714-1724, 2022.
2. D. Pilori et al., "Real-Time Monitoring of the Impact of Cascaded Wavelength-Selective Switches in Digital Coherent Receivers," *CLEO 2020*, paper SW3L.2.
3. A. Hraghi et al., "Experimental Demonstration of Linear Inter-Channel Interference Estimation Based on Neural Networks," *IEEE Photonics Journal*, vol. 15, no. 2, pp. 1-6, April 2023.
4. A. E. Pérez et al., "Spectral Spacing Estimation in Gridless Nyquist-WDM Systems using Local Binary Patterns," *IEEE IPC 2021*.
5. N. P. Puentes et al., "Deep Learning Approach to Estimate Interchannel Interference in gridless Nyquist-WDM Systems," *FIO+LS 2022*, paper JW5B.55.
6. X. Zhou and C. Xie, "Timing Synchronization in Coherent Optical Transmission Systems," in *Enabling Technologies for High Spectral-efficiency Coherent Optical Communication Networks*, Wiley, 2016, pp.355-394.
7. P. Stoica and R. L. Moses, "Spectral analysis of signals", vol. 452, Pearson Prentice Hall, 2005.
8. M.D. McKay et al., "A comparison of three methods for selecting values of input variables in the analysis of output from a computer code," *Technometrics* 42.1 (2000): 55-61.